Electrostatic co-assembly of $FePS_3$ nanosheets and surface functionalized BCN heterostructure for hydrogen evolution reaction

Abhinandan Patra[a], K Pramoda[a], Shridhar Hegde[a], Aravind K[a], Kseniia Mosina[b], Zdenek Sofer[b], Chandra Sekhar Rout[a*]

[a]*Centre for Nano and Material Sciences, Jain (Deemed–to–be University), Jain Global Campus, Kanakapura Road, Bangalore – 562112, Karnataka, India.*

[b] *Dept. of Inorganic Chemistry, University of Chemistry and Technology Prague, Technicka 5, 166 28 Prague 6, Czech Republic.*

E-mail: Corresponding author: [a*] *r.chandrasekhar@jainuniversity.ac.in;*
[a*]csrout@gmail.com

Formula used to calculate the electrochemical active surface area (ECSA), roughness factor (Rf), the double layer capacitance (Cdl), mass activity (MA), specific activity (SA) are given below along with the parameters and their designated symbols.[1-5]

1. $ECSA = \frac{C_{dl}}{C_s}$
2. $R_f = \frac{ECSA}{geometrical\ area\ of\ the\ electrode}$
3. $MA = \frac{j}{m}$
4. $SA = \frac{j}{m.10.S_{BET}}$

Here,

C_s = specific capacitance 0.04 mF/cm^2 in acidic condition

Geometrical area of the electrode = 0.0706 cm^2

j = current density in mA/cm^2

m = mass loading per geometrical active area in mg/cm^2

S_{BET} = surface area of the catalysts obtained from BET surface area analysis

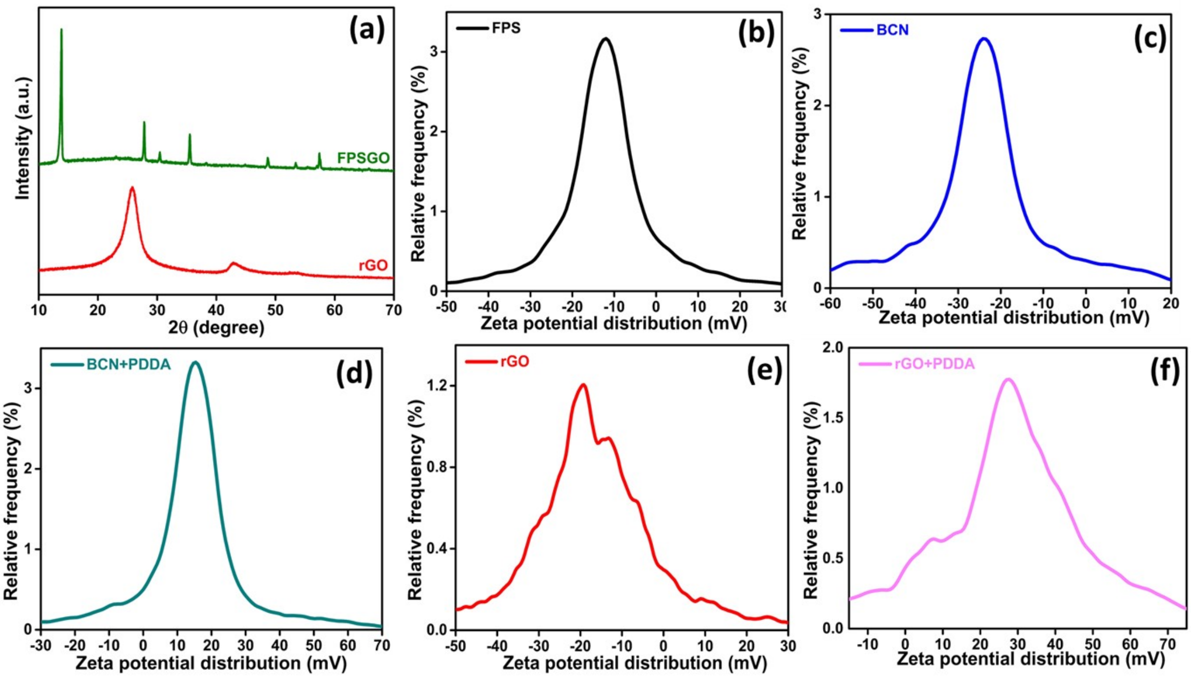

Fig-S1: (a) XRD pattern of rGO and FPSGO and (b) to (f) zeta potential electrokinetic measurements of FPS, BCN, BCN+PDDA, rGO and rGO+PDDA respectively.

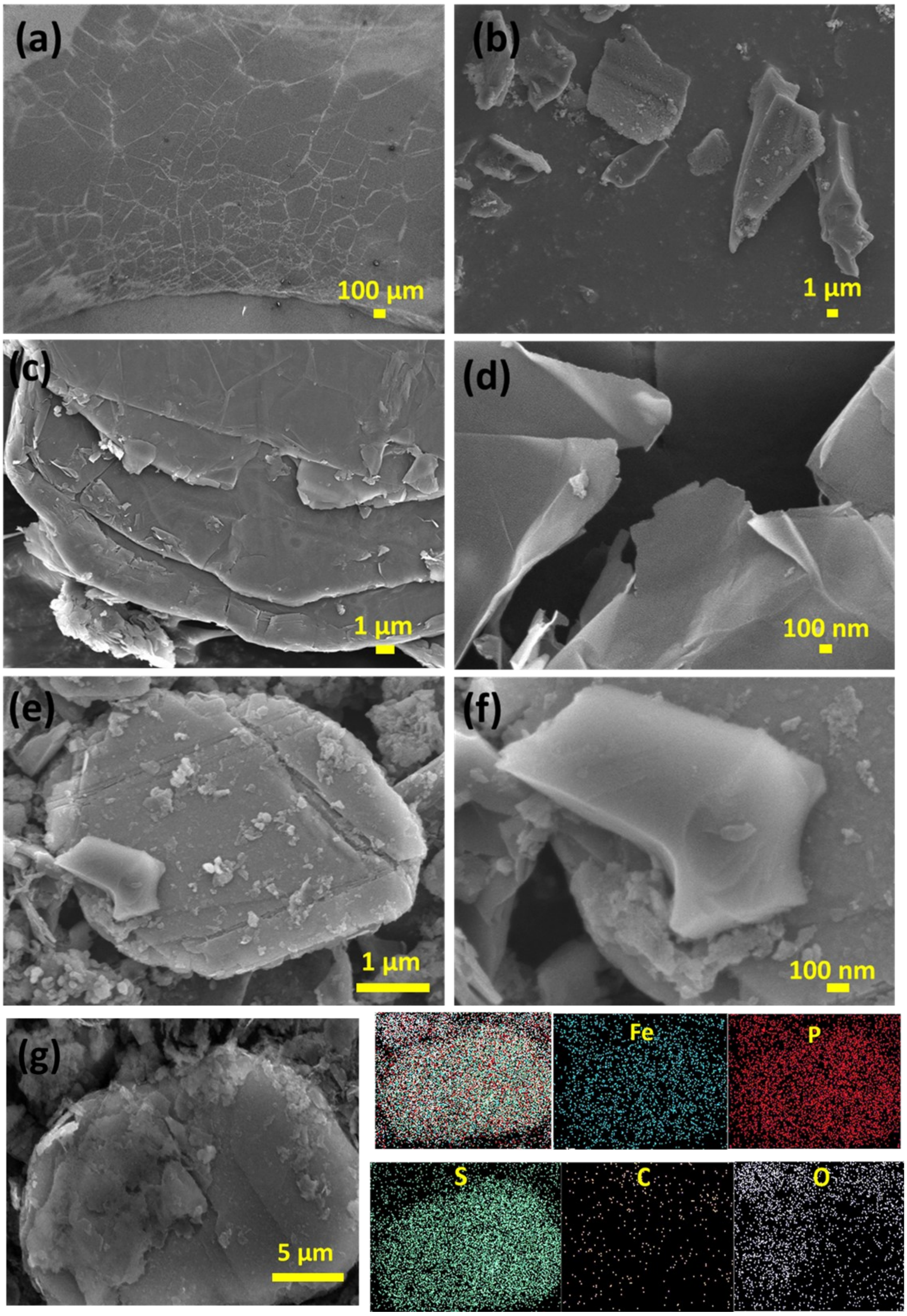

Fig-S2: FESEM images of (a) FPS crystal, (b) BCN nanosheets, (c) and (d) rGO sheets, (e) and (f) FPSGO and (g) EDAX mapping of FPSGO with individual elements.

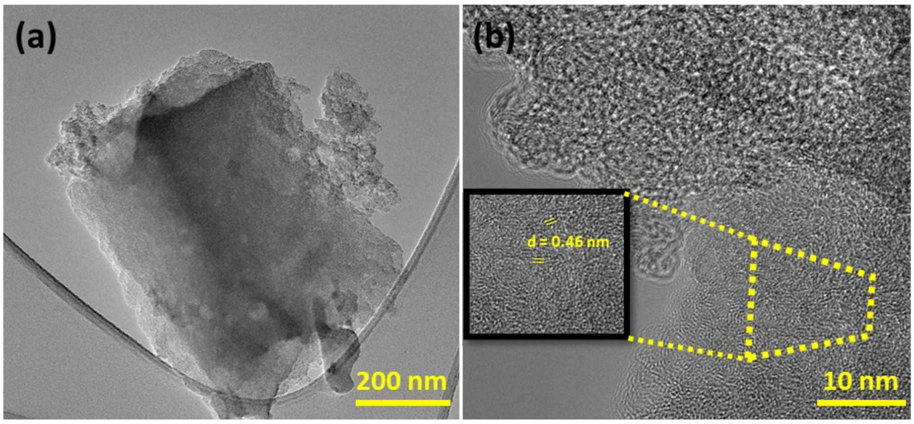

Fig-S3: (a) TEM and (b) HRTEM images of BCN.

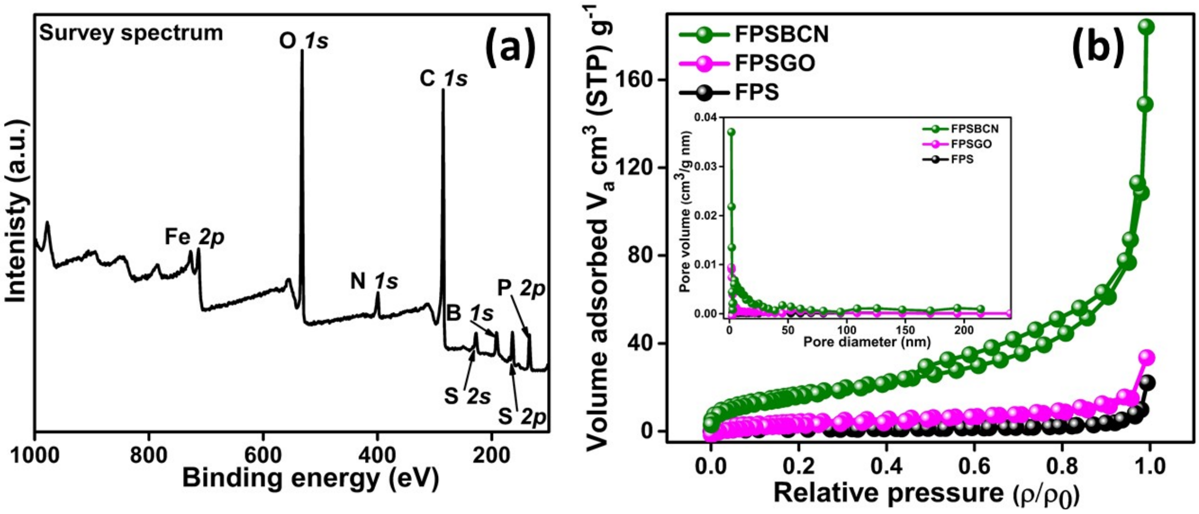

Fig-S4: (a) Survey spectra of FPSBCN and (b) BET surface area analysis of FPSBCN, FPSGO and FPS with inset image showing the graph of pore size distribution.

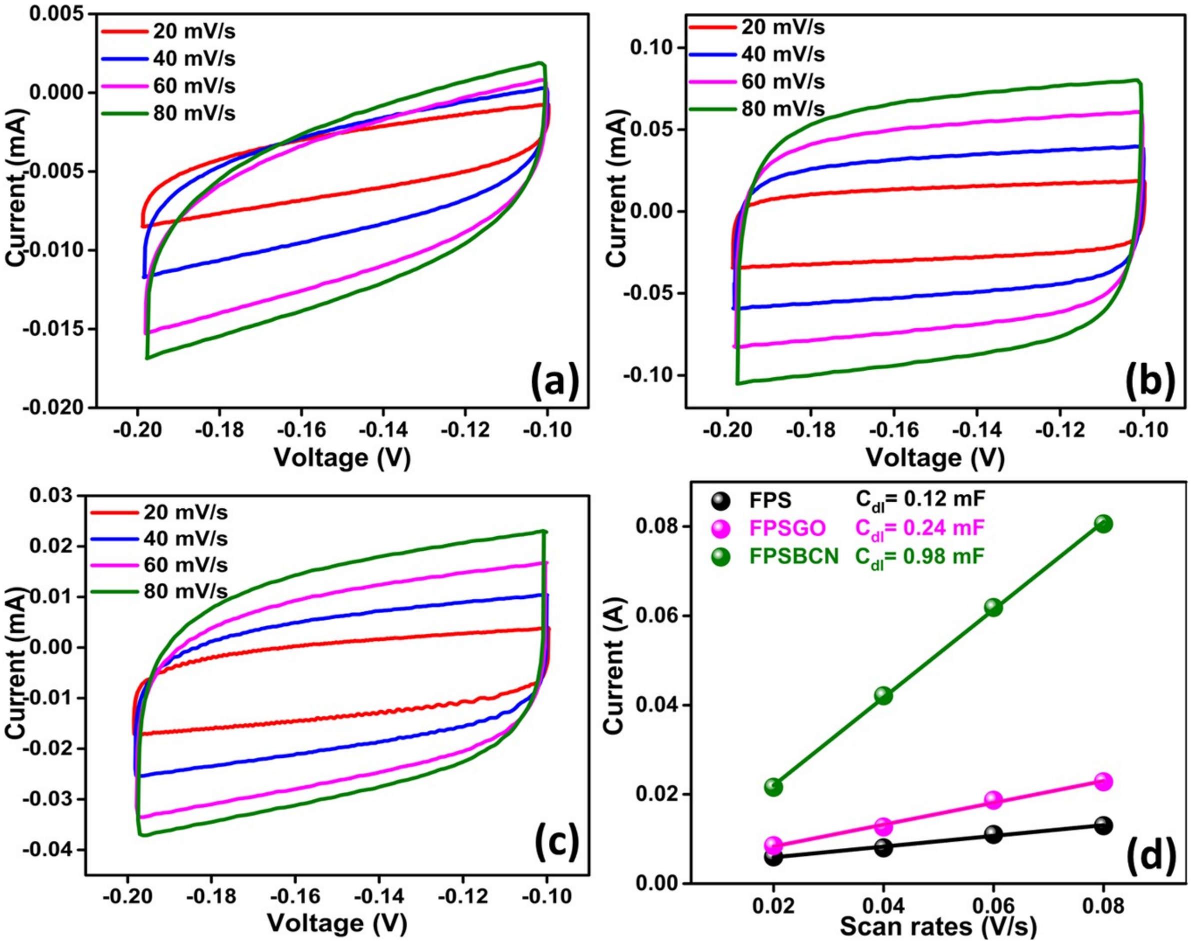

Fig-S5: CV measurements in -0.2 to -0.1 V; (a) FPS, (b) FPSGO, (c) FPSBCN and (d) evaluation of double layer capacitance from variation of current with scan rates.

Material code	Value of Zeta potential (mV)
FPS	-12.8
BCN	-22.6
BCN+PDDA	15.9
rGO	-14.2
FPSGO	24.5

Table-ST1: Zeta potential values of the catalysts in tabular form.

Material code	Surface area (m^2/g)	Pore volume (cm^3/g)	Pore diameter (nm)
FPS	3	0.029	35.64
FPSGO	18	0.049	11.23
FPSBCN	63	0.25	15.40

Table-ST2: BET surface area, pore volume and mean pore diameter of the catalysts in tabular form.

Material code	C_{dl} (mF)	ECSA (cm^2)	R_f	Mass activity (A/g)	Specific activity (mA/cm^2)
FPS	0.12	3	42.49	0.63	0.02
FPSGO	0.24	6	84.98	4.28	0.023
FPSBCN	0.98	24.5	347.02	119.29	0.189

Table ST3: C_{dl}, ECSA, R_f, mass activity and specific activity of the catalysts in tabular form

Serial No.	Material code	Electrolyte	Overpotential (mV)	Tafel (mV/dec)	Reference
1	B,N:Mo_2C@BCN	1 M KOH	100	62	6
2	BCN nanotube	0.5 M H_2SO_4	216	92	7
3	CoS_2@BCN	1 M KOH	376	130	8
4	$FePS_3$ nanosheets	0.5 M H_2SO_4	139	94	9
5	Co-$FePS_3$ nanosheets	1 M KOH	170	80	10
6	N-$FePS_3$ nanosheets	1 M KOH	267	163	11
7	MoS_2@$FePS_3$	0.5 M H_2SO_4	127	107	12
8	Cu-BCN composite	0.5 M H_2SO_4	125	114.5	13
9	β-Mo_2C@BCN	0.5 M H_2SO_4	140	103	14
10	FeCoMnNi-MOF	0.5 M H_2SO_4	108	73	15
11	Co-MOF	0.5 M H_2SO_4	44	45	16
12	Polyoxometalate	1 M KOH	131	51	17
13	Ni and Co-MOF	0.5 M H_2SO_4	350	60	18
10	**$FePS_3$@BCN**	**0.5 M H_2SO_4**	**186**	**41**	**This work**

Table-ST4: Comparison table of present catalysts with recent literature

References

1
A. Alinezhad, L. Gloag, T. M. Benedetti, S. Cheong, R. F. Webster, M. Roelsgaard, B. B. Iversen, W. Schuhmann, J. J. Gooding and R. D. Tilley, *Journal of the American Chemical Society*, 2019, **141**, 16202–16207.
2
A. Patra, R. Samal and C. S. Rout, *Catalysis Today*, DOI:https://doi.org/10.1016/j.cattod.2022.07.021.
3
L. Wu and J. P. Hofmann, *ACS Energy Letters*, 2021, **6**, 2619–2625.

4
Y. Shi, D. Zhang, H. Miao, X. Wu, Z. Wang, T. Zhan, J. Lai and L. Wang, *Science China Chemistry*, 2022, **65**, 1829–1837.
5
J. Zhang, L. Zhao, A. Liu, X. Li, H. Wu and C. Lu, *Electrochimica Acta*, 2015, **182**, 652–658.
6
M. A. R. Anjum, M. H. Lee and J. S. Lee, *ACS Catalysis*, 2018, **8**, 8296–8305.
7
H. Tabassum, R. Zou, A. Mahmood, Z. Liang and S. Guo, *Journal of Materials Chemistry A*, 2016, **4**, 16469–16475.
8
P. Borthakur, P. K. Boruah, M. R. Das, M. M. Ibrahim, T. Altalhi, H. S. El-Sheshtawy, S. Szunerits, R. Boukherroub and M. A. Amin, *ACS Applied Energy Materials*, 2021, **4**, 1269–1285.
9
Z. Yu, J. Peng, Y. Liu, W. Liu, H. Liu and Y. Guo, *Journal of Materials Chemistry A*, 2019, **7**, 13928–13934.
10
S. Wang, B. Xiao, S. Shen, K. Song, Z. Lin, Z. Wang, Y. Chen and W. Zhong, *Nanoscale*, 2020, **12**, 14459–14464.
11
H. Zhang, Y. Qiu, S. Zhang, Q. Liu, J. Luo and X. Liu, *Ionics*, 2022, **28**, 3927–3934.
12
H. Huang, J. Song, D. Yu, Y. Hao, Y. Wang and S. Peng, *Applied Surface Science*, 2020, **525**, 146623.
13
M. M. Hasan, G. E. Khedr, F. Zakaria and N. K. Allam, *ACS Applied Energy Materials*, 2022, **5**, 9692–9701.
14
M. A. R. Anjum, M. H. Lee and J. S. Lee, *Journal of Materials Chemistry A*, 2017, **5**, 13122–13129.
15
M. Zhang, W. Xu, T. Li, H. Zhu and Y. Zheng, *Inorganic Chemistry*, 2020, **59**, 15467–15477.
16
Y.-P. Wu, W. Zhou, J. Zhao, W.-W. Dong, Y.-Q. Lan, D. Li, C. Sun and X. Bu, *Angewandte Chemie*, 2017, **56**, 13001–13005.
17
Y. Zheng and X. Xu, *ACS Applied Materials & Interfaces*, 2020, **12**, 53739–53748.
18
V. V. Khrizanforova, R. P. Shekurov, Vasili Miluykov, Mikhail Khrizanforov, V. Bon, S. Kaskel, A. T. Gubaidullin, O. G. Sinyashin and Y. H. Budnikova, *Dalton Transactions*, 2020, **49**, 2794–2802.